

Sparse Array Beamforming Design for Wideband Signal Models

Syed A. Hamza, *Member, IEEE* and Moeness G. Amin, *Fellow, IEEE*

Abstract—We develop sparse array receive beamformer design methods achieving maximum signal-to-interference plus noise ratio (MaxSINR) for wideband sources and jammers. Both tapped delay line (TDL) filtering and the DFT realizations to wideband array processing are considered. The array sparsity stems from the limited number of available RF transmission chains that switch between the sensors, thereby configuring different arrays at different times. The sparse array configuration design problem is formulated as a quadratically constraint quadratic program (QCQP) and solved by using SDR (semidefinite relaxation). A computationally viable approach through SCA (successive convex relaxation) is also pursued. In order to realize an implementable design, in presence of missing autocorrelation lags, we propose parameter-free block Toeplitz matrix completion to estimate the received data correlation matrix across the entire array aperture. It is shown that the optimum wideband sparse array effectively utilizes the array aperture and provides considerable performance improvement over suboptimal array topologies.

Index Terms—Sparse arrays, DFT, TDL, MaxSINR, QCQP, SDR, SCA, wideband receive beamforming, Toeplitz matrix completion

I. INTRODUCTION

Wideband systems can deliver accurate target localization for radar systems [3], provide diversity, reliability and anti jamming capabilities to the wireless communication systems and signal enhancement for microphone arrays [4], [5], whereas the UWB (Ultra-wideband) systems play a major role in high resolution imaging in medical imaging [6], [7].

Beamforming techniques for wideband signals either involve a fixed design such as a frequency invariant beamformer or an adaptive design based on the linearly constrained minimum variance (LCMV) beamformer [8], [9]. Irrespective of the design criterion, the wideband beamformers are typically implemented jointly in the spatial and temporal domains, as shown in Fig. 1. This spatio-temporal processing is often realized through two different schemes, namely, the tapped delay line (TDL) filtering or subband processing like DFT. For the former, an L TDL filter is assumed for each sensor, and the received data at each sampling instant is processed for all sensors jointly [10], [11]. In the DFT implementation scheme, the data at each sensor is buffered and transformed to the

frequency domain by L -point DFT. Once expressed in terms of narrowband signals, optimal beamforming is performed in each DFT bin. The DFT implementation is computationally more viable [12]–[14]. However, the TDL implementation scheme has an added advantage since buffering is not required and the spatio-temporal weight vector can be updated at each sampling instant. The TDL and DFT beamformers would render identical output signal if the corresponding beamformer weights are related through a DFT transformation. However, carrying the beamformer design, separately in each domain, doesn't warrant the beamformer weights forming strictly a DFT pair. Resultantly, the output could differ slightly for each implementation. To circumvent the computationally expensive TDL beamformer design, a DFT beamformer is rather optimized and the DFT transformation is subsequently used to obtain the TDL beamformer. This dual domain TDL implementation designed primarily in the DFT domain can yield adequate output performance in practice [15].

Sparse array design strives to optimally deploy sensors, essentially achieving desirable beamforming characteristics, lowering the system hardware costs and reducing the computational complexity. Sparse array design is known to yield considerable performance advantages under different design criteria for narrowband signal models. These criteria can largely be segregated into environment-independent and environment-dependent designs. The minimum redundancy arrays (MRA) and the structured sparse array configurations are cases of the former design. They seek to optimize the environment-blind design criterion to enable the DOA estimation of more sources than physical sensors [16]–[19]. More recently, the switched antenna and beam technologies have motivated the design for environment adaptive sparse arrays. The available sensors are switched according to changing environmental conditions, enabling optimum use of expensive transceiver chains [20]–[23]. Sparse array design based on Cramer-Rao lower bound (CRLB) minimization criterion was shown effective for DOA estimation schemes [24]. On the other hand, beamforming approaches typically implements MaxSINR criterion, yielding efficient adaptive performance that is dependent on the underlying operating environment [25]–[31].

Designing sparse arrays has proved to be particularly advantageous for wideband signal models, as it circumvents the contradicting design requirements posed by the frequency spread of the signal. On the one hand, the lower frequency end of the spectrum puts a minimum aperture constraint on the array to achieve certain resolution. On the other hand, the higher end of the spectrum dictates the minimum separation between consecutive sensor locations so as to avoid spatial

This work was supported by National Science Foundation (NSF) award AST-1547420. This paper was presented in part at the 52nd Asilomar Conference on Signals, Systems, and Computers, Oct 2018 [1] and in part at the IEEE Radar Conference, Boston, MA, April 2019 [2]. (Corresponding author: Syed A. Hamza)

Syed A. Hamza is with the School of Engineering, Widener University PA and Moeness Amin is with the Center for Advanced Communications, College of Engineering, Villanova University, Villanova, PA 19085-1681 USA (e-mail: shamza@widener.edu; moeness.amin@villanova.edu).

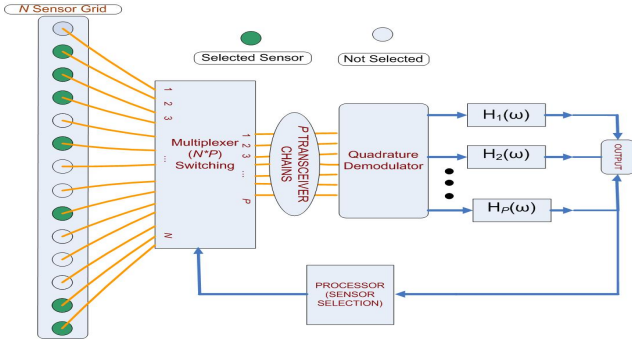


Fig. 1: Block Diagram of sparse array wideband processing.

aliasing, consequently, resulting in the oversampling of the lower frequency content. For a limited number of available sensors, wideband sparse array design can, in essence, yield improved performance in many design applications by offering more control over beampattern characteristics for all frequencies of interest [32]–[35]. Many different metrics, such as frequency invariant beampattern synthesis, robust beampattern design and side-lobe level control have been proposed for optimal wideband sparse array beamforming [34], [36]–[39]. For instance, simulated annealing has been applied in [38] to achieve the desired peak sidelobe levels, while jointly optimizing the beamformer weights and sensor locations. Frequency invariant beampattern optimization for wideband sparse array design employing compressive sensing (CS) technique has been implemented in [40]. The authors therein, invoked sparsity in the temporal and spatial domains, simultaneously, in an attempt to decrease the overall processing complexity.

In this paper, we examine the Capon based MaxSINR sparse array design from both the DFT and TDL filtering realization perspectives. We consider a switched array adaptive beamformer design which is fundamentally different as compared to the aforementioned wideband performance metrics that optimize a prefixed receive beampattern for certain sector/frequencies of interest, independent of the received data statistics. We examine environment-dependent sparse arrays that maximize the SINR for frequency spread source operating in wideband jamming environments. The objective of the populated and the sparse wideband beamformers is fundamentally the same; minimization of noise and interference signals at the array output while simultaneously maintaining a desired response in the direction of interest. We adopt a Capon based methodology for enhancing the signal power for the desired source operating in an interference active environment. Capon method is a well known linear constraint beamforming approach that rejects the interference and maximizes the output SINR [41]. It provides superior estimation accuracy but assumes the exact knowledge or estimated version of the received data correlation matrix across the entire array aperture. The latter is the case in many key applications in radar signal processing and medical imaging [1], [2], [42], [43]. This assumption, however, cannot be readily made for sparse array configurations.

We pose the design problem as optimally selecting P sensors out of N possible equally spaced locations. For

the scope of this paper, we ignore any mutual coupling or sensor failure possibilities that could arise due to the closely spaced perspective locations on the grid. Each sensor has an associated L TDL or L point DFT filtering to jointly process the signal in the temporal and spatial domains. Our approach is a natural extension of Capon beamforming at the receiver and amounts to maximizing the SINR over all possible sparse array configurations. In the case of the TDL realization, we select those sensors that maximize the principal eigenvalue of the product of the inverse of received data correlation matrix and the desired source correlation matrix [44]. For the DFT implementation scheme, the maximization is performed over all DFT bins. In either case, it is an NP hard optimization problem. In order to realize convex relaxation and avoid the computational burden of applying the singular value decomposition (SVD) for each possible configuration, we solve the underlying problem using constrained minimization based approach. We consider two different optimization approaches, namely, the semidefinite relaxation (SDR) and successive convex approximation (SCA). For SDR-based approach, we pose the problem as quadratically constraint quadratic program (QCQP) with weighted $l_{1-\infty}$ -norm squared to promote group sparsity. An eigenvector based iterative methodology is adopted to promote group sparsity and ensure that only P sensors are finally selected. It is noted that the re-weighted $l_{1-\infty}$ -norm squared relaxation is shown to be effective for reducing the number of sensors in multicast transmit beamforming [29]. However, owing to the computational complexity associated with the SDR approach, we alternatively pose the problem as successive convex relaxation (SCA) that approximates the problem iteratively by first order gradient approximation [45]. The proposed algorithms are suitable for moderate-size antenna systems to enable real time applications wherein the environment largely stays stationary relative to the time required for sparse configurability.

In order to enable a data-dependent design for sparse array wideband beamforming, we require knowledge of the received data correlation matrix corresponding to the full array aperture. With only few active sensors at any time instant, it is infeasible to assume such knowledge due to missing correlation entries. We circumvent this problem by employing a low rank block Toeplitz matrix completion scheme to interpolate the missing correlation entries. Subsequently, the interpolated data correlation matrix is input to the proposed sparse optimization algorithms. We demonstrate the offerings of the proposed sparse array design utilizing matrix completion under limited data snapshots by comparing its performance with that achieved through enumeration.

The rest of the paper is organized as follows: In the next section, we state the problem formulation for maximizing the output SINR under wideband source signal model by elucidating the TDL and DFT signal model. Section III deals with the optimum sparse array design by semidefinite relaxation as well as successive convex relaxation to obtain the optimum P sparse array geometry. Section IV discusses the block Toeplitz matrix completion approach for a conceivable sparse array design from an implementation perspective. Design examples and conclusion follow at the end.

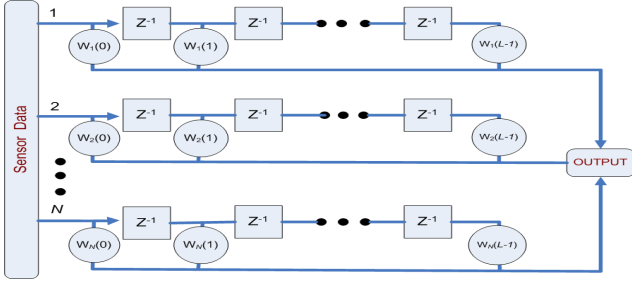


Fig. 2: TDL realization of wideband beamforming.

II. PROBLEM FORMULATION

Consider a single desired source and Q interfering source signals impinging on a linear array with N uniformly placed sensors. The Nyquist sampled received baseband signal $\mathbf{x}(n) \in \mathbb{C}^N$ at time instant n is, therefore, given by,

$$\mathbf{x}(n) = \mathbf{s}(n) + \sum_{k=1}^Q \mathbf{i}_k(n) + \mathbf{v}(n), \quad (1)$$

where $\mathbf{s}(n) \in \mathbb{C}^N$ is the contribution from the desired signal located at θ_s , $\mathbf{i}_k(n)$ is the k th interfering signal vectors corresponding to the respective direction of arrival, θ_k , and $\mathbf{v}(n)$ is the spatially uncorrelated sensor array output noise.

A. TDL Implementation scheme

We assume a TDL of length L associated with each sensor, as shown in Fig. 2. The symbol z^{-1} denotes the time delay and $w_k(m)$ is the beamforming weight for the k th sensor at m th sampling instant. We define a stacked vector $\mathbf{X} = [\mathbf{x}^T(n), \mathbf{x}^T(n-1), \dots, \mathbf{x}^T(n-L+1)]^T \in \mathbb{C}^{NL}$ containing the array data collected over L sampling instances ($(\cdot)^T$ denotes the transpose). Rewriting (1) in a compact way in terms of stacked vectors, we obtain,

$$\mathbf{X} = \mathbf{S} + \sum_{k=1}^Q \mathbf{I}_k + \mathbf{V} \quad (2)$$

Here, $\mathbf{S} = [\mathbf{s}^T(n), \mathbf{s}^T(n-1), \dots, \mathbf{s}^T(n-L+1)]^T$ and similarly \mathbf{I}_k and \mathbf{V} are defined, respectively, as interference and noise stacked vectors. The received signal \mathbf{X} is then combined linearly to maximize the output SINR. The output signal $y(n)$ of the optimum beamformer for maximum SINR is given by [44],

$$y(n) = \mathbf{w}_o^H \mathbf{X}, \quad (3)$$

where \mathbf{w}_o is the solution of the following optimization problem,

$$\begin{aligned} & \underset{\mathbf{w} \in \mathbb{C}^{NL}}{\text{minimize}} && \mathbf{w}^H \mathbf{R}_n \mathbf{w} \\ & \text{s.t.} && \mathbf{w}^H \mathbf{R}_s \mathbf{w} = 1 \end{aligned} \quad (4)$$

The $w_k(m)$ beamforming weight (shown in Fig. 2) maps to the $(N(m) + k)$ th element of the stacked beamformer \mathbf{w} ($m \in 0, 1, \dots, L-1$, $k \in 1, 2, \dots, N$). Here, $(\cdot)^H$ denotes Hermitian transpose, $\mathbf{R}_s = E(\mathbf{S}\mathbf{S}^H) \in \mathbb{C}^{NL \times NL}$ is the desired signal correlation matrix. Likewise, \mathbf{R}_n is the correlation matrix associated with interference and noise stacked vectors.

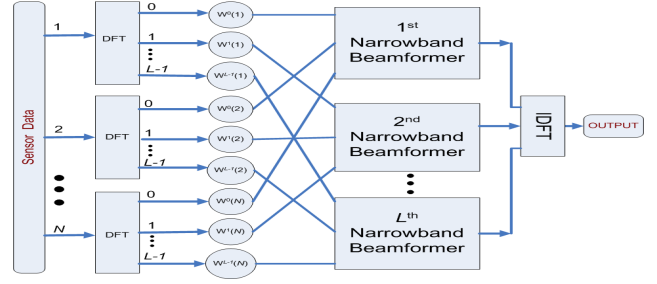


Fig. 3: DFT implementation of wideband beamforming.

In the case of spatial spread or wideband source signal, the correlation matrix is given by [10],

$$\mathbf{R}_s = \int_{B_s} \int_{\Theta_s} \sigma_{\theta_s}^2(\omega) \mathbf{a}(\theta_s, \omega) \mathbf{a}^H(\theta_s, \omega) d\theta_s d\omega \quad (5)$$

Here, $\sigma_{\theta_s}^2(\omega)$ is the signal power as a function of θ_s and ω , Θ_s and B_s are the spatial and spectral supports of the desired source signal. We only consider point sources with no significant spatial extent, hence rewriting (5) as follows,

$$\mathbf{R}_s = \int_{B_s} \sigma_{\theta_s}^2(\omega) \mathbf{a}(\theta_s, \omega) \mathbf{a}^H(\theta_s, \omega) d\omega \quad (6)$$

The space-time steering vector $\mathbf{a}(\theta_s, \omega) \in \mathbb{C}^{NL}$, corresponding to the source signal, can be represented as a Kronecker product (\otimes),

$$\mathbf{a}(\theta_s, \omega) = \boldsymbol{\phi}_\omega \otimes \mathbf{a}_{\theta_s}(\omega), \quad (7)$$

with,

$$\begin{aligned} \boldsymbol{\phi}_\omega &= [1 \ e^{j(\pi\omega/\omega_{max})} \ \dots \ e^{j(\pi\omega/\omega_{max})(L-1)}]^T, \\ \mathbf{a}_{\theta_s}(\omega) &= [1 \ e^{j(2\pi/\lambda_\omega)d\cos(\theta_s)} \ \dots \ e^{j(2\pi/\lambda_\omega)d(N-1)\cos(\theta_s)}]^T \\ &= [1 \ e^{j\pi(\frac{\omega_c+\omega}{\Omega_{max}})\cos(\theta_s)} \ \dots \ e^{j\pi(\frac{\omega_c+\omega}{\Omega_{max}})(N-1)\cos(\theta_s)}]^T, \end{aligned} \quad (8)$$

where λ_ω is the wavelength corresponding to $\omega_c + \omega$, ω and ω_c represent the baseband source angular frequency and the carrier angular frequency respectively, and ω_{max} is the maximum source baseband angular frequency. The data is sampled temporally at the Nyquist rate for a given signal bandwidth. Similarly, we set the inter-element spacing $d = \lambda_{min}/2$ to avoid spatial aliasing corresponding to the highest spatial angular frequency $\Omega_{max} = \omega_c + \omega_{max}$, where λ_{min} is the wavelength corresponding to Ω_{max} . The correlation matrix $\mathbf{R}_k \in \mathbb{C}^{NL \times NL}$ for the interferer \mathbf{i}_k is defined according to (6) with respect to θ_k and B_k . The sensor noise correlation matrix, $\mathbf{R}_v = \sigma_v^2 \mathbf{I} \in \mathbb{C}^{NL \times NL}$ assumes spatially and temporally uncorrelated noise $\mathbf{v}(n)$ with variance σ_v^2 . The problem in (4) can be written equivalently by replacing $\mathbf{R}_n = \sum_{k=1}^Q \mathbf{R}_k + \mathbf{R}_v$ with $\mathbf{R} = \mathbf{R}_s + \mathbf{R}_n$ as follows [44],

$$\begin{aligned} & \underset{\mathbf{w} \in \mathbb{C}^{NL}}{\text{minimize}} && \mathbf{w}^H \mathbf{R} \mathbf{w} \\ & \text{s.t.} && \mathbf{w}^H \mathbf{R}_s \mathbf{w} \geq 1 \end{aligned} \quad (10)$$

The equality constraint is relaxed in (10) due to the inclusion of the constraint autocorrelation matrix as part of the objective function, thereby the optimal solution always converges at the equality constraint. The analytical solution

of the above optimization problem exists and is given by $\mathbf{w}_o = \mathcal{P}\{\mathbf{R}_n^{-1}\mathbf{R}_s\} = \mathcal{P}\{\mathbf{R}^{-1}\mathbf{R}_s\}$. The operator $\mathcal{P}\{\cdot\}$ computes the principal eigenvector of its argument. Substituting $\mathbf{w}_o = \mathcal{P}\{\mathbf{R}_n^{-1}\mathbf{R}_s\}$ into the SINR formula yields the corresponding optimum output $SINR_o$ (Λ_{max} denotes the maximum eigenvalue of the matrix);

$$SINR_o = \frac{\mathbf{w}_o^H \mathbf{R}_s \mathbf{w}_o}{\mathbf{w}_o^H \mathbf{R}_n \mathbf{w}_o} = \Lambda_{max}\{\mathbf{R}_n^{-1}\mathbf{R}_s\}, \quad (11)$$

which shows that the optimum beamformer for maximizing SINR is directly related to the desired and interference plus noise correlation matrices.

B. DFT Implementation scheme

Figure 3 shows the DFT implementation scheme of wideband array processing. The received signal $\mathbf{x}(n)$ is processed in the spectral domain by taking an L point DFT for the data received by k th sensor $x_k(n)$,

$$X_k^{(l)} = \sum_{p=0}^{L-1} x_k(n-p)(e^{-j\frac{2\pi}{L}})^{lp}, \quad l \in \{0, 1, \dots, L-1\} \quad (12)$$

Define a vector $\mathbf{X}^{(l)} \in \mathbb{C}^N$, containing the l th DFT bin data corresponding to each sensor (superscript (l) denotes the l th DFT bin),

$$\mathbf{X}^{(l)} = [X_1^{(l)}, X_2^{(l)}, \dots, X_N^{(l)}]^T \quad (13)$$

These samples are then combined linearly by the weight vector $\mathbf{w}^{(l)} \in \mathbb{C}^N$ such that,

$$y^{(l)} = \mathbf{w}^{(l)H} \mathbf{X}^{(l)}, \quad l \in \{0, 1, \dots, L-1\} \quad (14)$$

Subsequently, the overall beamformer output y is generated by taking the inverse DFT of $y^{(l)}$ across the L beamformers. The DFT implementation scheme seeks to maximize the output SINR for each frequency bin, yielding the optimum beamforming weight vector $\mathbf{w}_o^{(l)}$ as the solution of the following optimization problem,

$$\begin{aligned} & \text{minimize}_{\mathbf{w}^{(l)} \in \mathbb{C}^N} \sum_{l=0}^{L-1} \mathbf{w}^{(l)H} \mathbf{R}^{(l)} \mathbf{w}^{(l)} \\ & \text{s.t. } \mathbf{w}^{(l)H} \mathbf{R}_s^{(l)} \mathbf{w}^{(l)} \geq 1, \quad l \in \{0, 1, \dots, L-1\} \end{aligned} \quad (15)$$

The correlation matrix $\mathbf{R}^{(l)} = \mathbf{X}^{(l)}\mathbf{X}^{(l)H}$ is the received correlation matrix for the l th processing bin. Similarly, the source correlation matrix $\mathbf{R}_s^{(l)}$ for the desired source impinging from direction of arrival θ_s is given by,

$$\mathbf{R}_s^{(l)} = \mathbf{S}^{(l)}\mathbf{S}^{(l)H} = \sigma_s^{(l)2} \mathbf{a}_{\theta_s}^{(l)} \mathbf{a}_{\theta_s}^{(l)H} \quad (16)$$

Here, $\mathbf{S}^{(l)}$ is the received data vector representing the desired source and $\sigma_s^{(l)2}$ denotes the power of this source in the l th bin, $\mathbf{a}_{\theta_s}^{(l)}$ is the corresponding steering vector for the source (DOA θ_s) and is defined as follows,

$$\begin{aligned} \mathbf{a}_{\theta_s}^{(l)} = & [1 \ e^{j\pi(\frac{\Omega_{min} + l\Delta\omega}{\Omega_{max}})\cos(\theta_s)} \\ & \dots \ e^{j\pi(\frac{\Omega_{min} + l\Delta\omega}{\Omega_{max}})(N-1)\cos(\theta_s)}]^T \end{aligned} \quad (17)$$

Eq. (17) models the steering vector for the l th DFT bin, where Ω_{min} is the lower edge of the passband and $\Delta\omega = \frac{2w_{max}}{L}$ is the spectral resolution. The overall output SINR is given by averaging the SINR over all DFT bins. Similar to the TD-L, the DFT implementation scheme determines the optimum sparse array geometry for enhanced MaxSINR performance as explained in the following section.

III. OPTIMUM SPARSE ARRAY DESIGN

The problem of maximizing the principal eigenvalue for the P sensor selection is a combinatorial optimization problem. In this section, we assume that the full array data correlation matrix is known. However, Section IV explains the means to avoid this assumption through fully augmentable sparse array design or utilizing the matrix completion approach [46]–[48]. We first formulate the sparse array design for maximizing SINR in the case of wideband beamforming as an SDR. Owing to the high computational complexity of SDR, the problem is solved by SCA, for both the TD-L and DFT implementation schemes.

A. Semidefinite relaxation (SDR) for sparse solution

1) *TD-L Implementation scheme:* We assume that the sensor configuration remains the same within the observation time. In radar, this assumption amounts to selecting the same P sensors over the coherent processing interval (CPI). Therefore, the task is to select P entries from the first N elements of \mathbf{w} , and the same P entries from each subsequent block of N elements (there are L such blocks). Define $\mathbf{w}_k = [\mathbf{w}(k), \mathbf{w}(k+N), \dots, \mathbf{w}(k+N(L-1))] \in \mathbb{C}^L$ ($k \in \{1, \dots, N\}$) as the weights corresponding to TD-L of k th sensor. Then, in seeking sparse solution, the problem in (10) can be reformulated as follows,

$$\begin{aligned} & \text{minimize}_{\mathbf{w} \in \mathbb{C}^{NL}} \mathbf{w}^H \mathbf{R} \mathbf{w} + \bar{\mu} \left(\sum_{k=1}^N \|\mathbf{w}_k\|_q \right) \\ & \text{s.t. } \mathbf{w}^H \mathbf{R}_s \mathbf{w} \geq 1 \end{aligned} \quad (18)$$

Here, $\|\cdot\|_q$ denotes the q -norm of the vector, $\bar{\mu}$ is the sparsity regularization parameter. The mixed l_{1-q} norm regularization is known to thrive the group sparsity in the solution. In so doing, the above formulation enables the decision making on whether to collectively select or discard all the L sampling instances associated with the k th sensor. Therefore, structured group sparsity is essential for wideband beamformer, since the final sparse solution has to ensure that only PL out of NL spatio-temporal possible sampling instances are chosen through only P physical sensors. The relaxed problem expressed in the above equation induces group sparsity in the optimal weight vector without placing a hard constraint on the desired cardinality. The constrained minimization in (18) can be penalized instead by the weighted l_1 -norm function to further promote sparse solutions [49]–[51],

$$\begin{aligned} & \text{minimize}_{\mathbf{w} \in \mathbb{C}^{NL}} \mathbf{w}^H \mathbf{R} \mathbf{w} + \bar{\mu} \left(\sum_{k=1}^N \mathbf{u}^i(k) \|\mathbf{w}_k\|_q \right) \\ & \text{s.t. } \mathbf{w}^H \mathbf{R}_s \mathbf{w} \geq 1, \end{aligned} \quad (19)$$

Algorithm 1 SDR for the sparse wideband beamformer

Input: Sparse correlation matrices $\hat{\mathbf{R}}$ for TDL-SDR ($\hat{\mathbf{R}}^{(l)}$ for DFT-SDR), N, P, L, \mathbf{R}_s for TDL-SDR ($\mathbf{R}_s^{(l)}$ for DFT-SDR).

Output: MaxSINR beamformer against P active sensors.

Matrix Completion:

Estimate full data receive correlation matrix $\hat{\mathbf{R}}$ for TDL-SDR ($\hat{\mathbf{R}}^{(l)}$ for DFT-SDR).

Initialization:

Initialize ϵ, μ_{max} (upper limit of binary search), μ_{min} (lower limit of binary search), $\mathbf{U} =$ all ones matrix.

Appropriate value of μ is selected through the binary search to ensure P sensor selection.

while (Beamforming weight vector is not P sparse) **do**

Select $\mu = \frac{1}{2}(\mu_{max} + \mu_{min})$ (Binary search).

Run the SDR of (22) for TDL-SDR or (23) for DFT-SDR (Use either $\hat{\mathbf{R}}, \hat{\mathbf{R}}^{(l)}$ in-lieu of $\mathbf{R}, \mathbf{R}^{(l)}$).

Update \mathbf{U}^i according to (25).

Update μ_{max}/μ_{min} according to the binary search.

end while

Run SDR for reduced size correlation matrix corresponding to P sensors of $\tilde{\mathbf{W}}$ and $\mu = 0$, yielding, $\mathbf{w}_o = \mathcal{P}\{\mathbf{W}\}$ for TDL-SDR ($\mathbf{w}_o^{(l)} = \mathcal{P}\{\mathbf{W}^{(l)}\}$ for DFT-SDR).

return Optimal Beamformer \mathbf{w}_o -TDL-SDR ($\mathbf{w}_o^{(l)}$ -DFT-SDR)

where, $\mathbf{u}^i(k)$ is the k th element of re-weighting vector \mathbf{u}^i at the i th iteration. We choose the ∞ -norm for the q -norm and replace the weighted l_1 -norm function in (19) by the l_1 -norm squared function with a modified regularization parameter (μ instead of $\bar{\mu}$). This change does not affect the regularization property of the l_1 -norm [29]. The result is,

$$\begin{aligned} \underset{\mathbf{w} \in \mathbb{C}^{NL}}{\text{minimize}} \quad & \mathbf{w}^H \mathbf{R} \mathbf{w} + \mu \left(\sum_{k=1}^N \mathbf{u}^i(k) \|\mathbf{w}_k\|_\infty \right)^2 \\ \text{s.t.} \quad & \mathbf{w}^H \mathbf{R}_s \mathbf{w} \geq 1 \end{aligned} \quad (20)$$

The SDR of the above problem is realized by substituting $\mathbf{W} = \mathbf{w} \mathbf{w}^H$. The quadratic function, $\mathbf{w}^H \mathbf{R} \mathbf{w} = \text{Tr}(\mathbf{w}^H \mathbf{R} \mathbf{w}) = \text{Tr}(\mathbf{R} \mathbf{w} \mathbf{w}^H) = \text{Tr}(\mathbf{R} \mathbf{W})$, where $\text{Tr}(\cdot)$ is the trace of the matrix. Similarly, we replace the regularization term in (20) by $\text{Tr}(\mathbf{U}^i \tilde{\mathbf{W}})$, with $\mathbf{U}^i = \mathbf{u}^i (\mathbf{u}^i)^T$ and $\tilde{\mathbf{W}}$ being the auxiliary matrix implementing ∞ -norm as follows [29], [52], [53],

$$\begin{aligned} \underset{\mathbf{W} \in \mathbb{C}^{NL \times NL}, \tilde{\mathbf{W}} \in \mathbb{R}^{N \times N}}{\text{minimize}} \quad & \text{Tr}(\mathbf{R} \mathbf{W}) + \mu \text{Tr}(\mathbf{U}^i \tilde{\mathbf{W}}) \\ \text{s.t.} \quad & \text{Tr}(\mathbf{R}_s \mathbf{W}) \geq 1, \\ & \tilde{\mathbf{W}} \geq |\mathbf{W}_{ll}|, \quad l \in \{0, \dots, L-1\}, \\ & \mathbf{W} \succeq 0, \text{Rank}(\mathbf{W}) = 1 \end{aligned} \quad (21)$$

The operator ‘ $|\cdot|$ ’ returns the element wise absolute values of the entries of the matrix, ‘ \geq ’ is the element wise comparison and ‘ \succeq ’ represents the generalized matrix inequality, implementing the positive semidefinite constraint, $\mathbf{W}_{ll} \in \mathbb{C}^{N \times N}$ is the l th diagonal block matrix of \mathbf{W} . We note that the

solution matrix \mathbf{W} is Hermitian and therefore, it is sufficient to constrain the upper or lower triangular entries of \mathbf{W}_{ll} while forcing $\tilde{\mathbf{W}}$ to be symmetric matrix. In so doing, we reduce the inequality constraints and decrease the run time substantially. In addition, we drop rank constraint in (21) which is non convex, resulting in the following SDR,

$$\begin{aligned} \underset{\mathbf{W} \in \mathbb{C}^{NL \times NL}, \tilde{\mathbf{W}} \in \mathbb{R}^{N \times N}}{\text{minimize}} \quad & \text{Tr}(\mathbf{R} \mathbf{W}) + \mu \text{Tr}(\mathbf{U}^i \tilde{\mathbf{W}}), \\ \text{s.t.} \quad & \text{Tr}(\mathbf{R}_s \mathbf{W}) \geq 1, \\ & \tilde{\mathbf{W}} \geq |\tilde{\mathbf{W}}_{ll}|, \quad l \in \{0, 1, \dots, L-1\}, \\ & \tilde{\mathbf{W}} = \tilde{\mathbf{W}}^T, \quad \mathbf{W} \succeq 0. \end{aligned} \quad (22)$$

Here, Δ represents the upper or lower triangular entries of the matrix.

2) *DFT Implementation scheme:* The DFT implementation scheme for sparse array design is achieved by starting from (15) and following similar steps of the TDL. The group sparsity is invoked as the data in each DFT bin requires the underlying array configuration to remain the same for processing over all DFT bins. The SDR is finally realized as follows,

$$\begin{aligned} \underset{\mathbf{W}^{(l)} \in \mathbb{C}^{N \times N}, \tilde{\mathbf{W}} \in \mathbb{R}^{N \times N}}{\text{minimize}} \quad & \sum_{l=0}^{L-1} \text{Tr}(\mathbf{R}^{(l)} \mathbf{W}^{(l)}) + \mu \text{Tr}(\mathbf{U}^i \tilde{\mathbf{W}}) \\ \text{s.t.} \quad & \text{Tr}(\mathbf{R}_s^{(l)} \mathbf{W}^{(l)}) \geq 1, \quad l \in \{0, 1, \dots, L-1\}, \\ & \tilde{\mathbf{W}}^{(l)} \geq |\tilde{\mathbf{W}}^{(l)}|, \quad l \in \{0, 1, \dots, L-1\}, \\ & \tilde{\mathbf{W}} = \tilde{\mathbf{W}}^T, \quad \mathbf{W} \succeq 0. \end{aligned} \quad (23)$$

It is evident from (22) and (23) that the dimensionality of the TDL implementation scheme is $NL \times NL$, whereas the DFT approach involves L unknown variables of dimensions $N \times N$.

3) *Unit rank promoting iteration:* Promoting sparse solutions iteratively would depend on careful selection of the regularization weighting matrix at each iteration. As suggested in [29], [51], the weighting matrix \mathbf{U}^i in (22) and (23) is initialized unweighted, i.e., a matrix of all ones. Afterwards, this matrix is iteratively updated in an inverse relationship to $\tilde{\mathbf{W}}$, which is related to the solution matrix \mathbf{W} from the previous iteration. This enables the beamforming weights having relatively lower magnitude to be penalized aggressively, hence encouraging them to go to zero in an iterative fashion. The parameter ϵ prevents the unwanted case of division by zero and also avoids the solution to converge to local minima as follows,

$$\mathbf{U}^{i+1}(m, n) = \frac{1}{\tilde{\mathbf{W}}^i(m, n) + \epsilon} \quad (24)$$

However, the solution matrix \mathbf{W} in the case of the TDL implementation scheme is not exactly rank one at initial iterations. The problem aggravates when the weight matrix is updated according to the above equation, inadvertently pushing the rank of \mathbf{W} to build up with each iteration. In this respect, updating \mathbf{U} according to (24) favors solutions of higher ranks, and, as such, fails to yield sparse configurations iteratively. To mitigate this problem, we propose a modified re-weighting

scheme that relies on updating the regularization weighting matrix that depends on the inverse of a rank 1 matrix \mathbf{Y} instead of $\tilde{\mathbf{W}}$ as follows,

$$\mathbf{U}^{i+1}(m, n) = \frac{1}{\mathbf{Y}^i(m, n) + \epsilon}, \quad (25)$$

where, $\mathbf{Y}^i = \mathbf{y}^i(\mathbf{y}^i)^T$, for $\mathbf{y}^i = \frac{1}{L} \sum_{l=1}^L (|\mathcal{P}\{\mathbf{W}_{ll}^i\}|)^2$. Clearly, \mathbf{Y}^i is a rank one matrix that is synthesized from the rank one approximation of each block diagonal matrix \mathbf{W}_{ll}^i . It is noted that \mathbf{W}_{ll}^i are the only entries of \mathbf{W} that are constrained by the SDR formulated in (22). Since \mathbf{W}_{ll}^i are the diagonal block matrices of the solution matrix \mathbf{W} , then sparsity is implicitly encouraged in \mathbf{W} by unit rank penalization. This modified re-weighting approach given by (25) effectively solves the optimum sparse array selection problem for the wideband beamforming. It is noted that the arbitrarily chosen sparsity parameter μ does not ensure the final solution to be exactly P sparse. In order to do so, the optimization problem should be solved against various values of μ . This is typically achieved by successively running the optimization and updating the values of μ through a binary search over the possible upper and lower limit of μ_{max}/μ_{min} , until the solution converges to P sensors [29]. The proposed algorithm for achieving the sparse optimal weight vector under the TDL and DFT implementation schemes is summarized in Algorithm 1.

B. Successive convex approximation (SCA)

1) *TDL Implementation scheme*: The problem in (10) can equivalently be rewritten by swapping the objective and constraint functions as follows,

$$\begin{aligned} & \underset{\mathbf{w} \in \mathbb{C}^{NL}}{\text{maximize}} \quad \mathbf{w}^H \mathbf{R}_s \mathbf{w} \\ & \text{s.t.} \quad \mathbf{w}^H \mathbf{R} \mathbf{w} \leq 1 \end{aligned} \quad (26)$$

Although this swapping operation allows the associated constraint to be convex, however it renders the objective function non convex. We note that the formulation in (26) doesn't have a trivial solution $\mathbf{w} = 0$, as the objective and constraint are coupled due to \mathbf{R}_s being part of \mathbf{R} . The maximization of the convex function is replaced by the minimization of the concave function. The transformation to the minimization problem will later enable carrying out the minimization based on P sparse solution. Rewriting (26) by reversing the sign of the desired source correlation matrix $\tilde{\mathbf{R}}_s = -\mathbf{R}_s$ as follows,

$$\begin{aligned} & \underset{\mathbf{w} \in \mathbb{C}^{NL}}{\text{minimize}} \quad \mathbf{w}^H \tilde{\mathbf{R}}_s \mathbf{w} \\ & \text{s.t.} \quad \mathbf{w}^H \mathbf{R} \mathbf{w} \leq 1 \end{aligned} \quad (27)$$

The beamforming weight vectors are generally complex valued, whereas the quadratic functions are real. This observation allows expressing the problem with only real variables and is typically accomplished by replacing the correlation matrix $\tilde{\mathbf{R}}_s$ by $\tilde{\mathbf{R}}_s$ and concatenating the beamforming weight vector accordingly [45],

$$\tilde{\mathbf{R}}_s = \begin{bmatrix} \text{real}(\tilde{\mathbf{R}}_s) & -\text{imag}(\tilde{\mathbf{R}}_s) \\ \text{imag}(\tilde{\mathbf{R}}_s) & \text{real}(\tilde{\mathbf{R}}_s) \end{bmatrix}, \tilde{\mathbf{w}} = \begin{bmatrix} \text{real}(\mathbf{w}) \\ \text{imag}(\mathbf{w}) \end{bmatrix} \quad (28)$$

Algorithm 2 SCA for the sparse wideband beamformer

Input: Sparse correlation matrices $\hat{\mathbf{R}}$ for TDL-SCA ($\hat{\mathbf{R}}^{(l)}$ for DFT-SCA), N, P, L, \mathbf{R}_s for TDL-SCA ($\mathbf{R}_s^{(l)}$ for DFT-SCA).

Output: MaxSINR beamformer against P active sensors.

Matrix Completion:

Estimate full data receive correlation matrix $\hat{\mathbf{R}}$ for TDL-SCA ($\hat{\mathbf{R}}^{(l)}$ for DFT-SCA).

Initialization:

Initialize $\mathbf{m}, b, \epsilon, \mu_{max}$ (upper limit of binary search), μ_{min} (lower limit of binary search), $\mu = 0, \mathbf{u}^i =$ all ones vector.

while (Solution does not converge for $\mu = 0$) **do**

 Run (31) for TDL-SCA or (32) for DFT-SCA.

end while

while (Beamforming weight vector is not P sparse) **do**

 Select $\mu = \frac{1}{2}(\mu_{max} + \mu_{min})$ (Binary search).

 Run (31) for TDL-SCA or (32) for DFT-SCA (Use $\hat{\mathbf{R}}$ or $\hat{\mathbf{R}}^{(l)}$ in-lieu of $\mathbf{R}, \mathbf{R}^{(l)}$ to synthesize $\tilde{\mathbf{R}}, \tilde{\mathbf{R}}^{(l)}$).

 (Also use the optimal non sparse solution from the previous while loop for \mathbf{m} and b).

 Update the regularization weighting parameter $\mathbf{u}^{i+1}(k) = \frac{1}{\|\tilde{\mathbf{w}}_k^i\|_2 + \epsilon}$.

 Update μ_{max}/μ_{min} according to the binary search.

end while

Run (31) for TDL-SCA or (32) for DFT-SCA, with reduced dimension corresponding to P sensors of $\tilde{\mathbf{w}}$ and $\mu = 0$, yielding, optimal weight vector.

return Optimal Beamformer \mathbf{w}_o -TDL-SCA ($\mathbf{w}_o^{(l)}$ -DFT-SCA)

Similarly, the received data correlation matrix \mathbf{R} is replaced by $\tilde{\mathbf{R}}$. The problem in (27) then becomes,

$$\begin{aligned} & \underset{\tilde{\mathbf{w}} \in \mathbb{R}^{2NL}}{\text{minimize}} \quad \tilde{\mathbf{w}}^T \tilde{\mathbf{R}}_s \tilde{\mathbf{w}} \\ & \text{s.t.} \quad \tilde{\mathbf{w}}^T \tilde{\mathbf{R}} \tilde{\mathbf{w}} \leq 1 \end{aligned} \quad (29)$$

We can then proceed to convexify the objective function by utilizing the first order approximation iteratively,

$$\begin{aligned} & \underset{\tilde{\mathbf{w}} \in \mathbb{R}^{2NL}}{\text{minimize}} \quad \mathbf{m}^i{}^T \tilde{\mathbf{w}} + b^i \\ & \text{s.t.} \quad \tilde{\mathbf{w}}^T \tilde{\mathbf{R}} \tilde{\mathbf{w}} \leq 1, \end{aligned} \quad (30)$$

The linearization coefficients \mathbf{m}^i and b^i are updated as, $\mathbf{m}^{i+1} = 2\tilde{\mathbf{R}}_s \tilde{\mathbf{w}}^i$, and $b^{i+1} = -\tilde{\mathbf{w}}^i{}^T \tilde{\mathbf{R}}_s \tilde{\mathbf{w}}^i$ (superscript i denotes the iteration number). Finally, to invoke sparsity in the beamforming weight vector, the re-weighted mixed l_{1-2} norm is adopted primarily for promoting group sparsity,

$$\begin{aligned} & \underset{\tilde{\mathbf{w}} \in \mathbb{R}^{2NL}}{\text{minimize}} \quad \mathbf{m}^i{}^T \tilde{\mathbf{w}} + b^i + \mu \left(\sum_{k=1}^N \mathbf{u}^i(k) \|\tilde{\mathbf{w}}_k\|_2 \right) \\ & \text{s.t.} \quad \tilde{\mathbf{w}}^T \tilde{\mathbf{R}} \tilde{\mathbf{w}} \leq 1 \end{aligned} \quad (31)$$

Here, $\tilde{\mathbf{w}}_k \in \mathbb{R}^{2L}$ are the beamforming weights corresponding to TDL of k th sensor. Discouraging a sensor ($\|\cdot\|_2$ denotes the l_2 norm) implies a simultaneous removal of both the real and

corresponding imaginary entries of all beamforming weights associated with the removed sensor [45].

2) *DFT implementation scheme*: The above formulation can be extended for the DFT implementation scheme as follows:

$$\begin{aligned} & \underset{\tilde{\mathbf{w}}^{(l)} \in \mathbb{R}^{2N}}{\text{minimize}} \sum_{l=0}^{L-1} (\{\mathbf{m}^{(l)}\}^i \tilde{\mathbf{w}}^{(l)} + \{b^{(l)}\}^i) + \mu \left(\sum_{k=1}^N \mathbf{u}^i(k) \|\tilde{\mathbf{w}}_k\|_2 \right) \\ & \text{s.t. } \tilde{\mathbf{w}}^{(l)T} \tilde{\mathbf{R}}^{(l)} \tilde{\mathbf{w}}^{(l)} \leq 1, \quad l \in \{0, 1, \dots, L-1\}, \end{aligned} \quad (32)$$

where $\tilde{\mathbf{w}}_k \in \mathbb{R}^{2L}$ contains the L DFT bins data for the k th sensor, $\{\mathbf{m}^{(l)}\}^i$ and $\{b^{(l)}\}^i$ are the approximation coefficients at the i th iteration for the desired source correlation matrix in the l th bin, with $\{\mathbf{m}^{(l)}\}^i = 2\tilde{\mathbf{R}}_s^{(l)}\{\tilde{\mathbf{w}}^{(l)}\}^i$, $\{b^{(l)}\}^i = -\{\tilde{\mathbf{w}}^{(l)}\}^i \tilde{\mathbf{R}}_s^{(l)}\{\tilde{\mathbf{w}}^{(l)}\}^i$. The initial estimates $\{\mathbf{m}^{(l)}\}^i$ and $\{b^{(l)}\}^i$ are calculated for the optimal non sparse solution. These parameters can be found by setting the sparsity parameter μ to zero. In so doing, the solution and the corresponding parameters $\{\mathbf{m}^{(l)}\}^i$ and $\{b^{(l)}\}^i$ converge to the optimal value against the full array elements. Using these values as initial conditions has proven appropriate in our design for recovering effective sparse solutions. The sparsity parameter μ is chosen according to the binary search over the possible range of μ to warrant the desired cardinality of the beamforming weight vector as explained before in section III-A3. The k th entry of re-weighting vector $\mathbf{u}^i(k)$ is updated according to $\mathbf{u}^{i+1}(k) = \frac{1}{\|\tilde{\mathbf{w}}_k^i\|_2 + \epsilon}$. The SCA for sparse array design for wideband beamforming is summarized in Algorithm 2.

C. Computational complexity

In general, QCQP of order M with T quadratic constraints can be solved to an arbitrary small accuracy ζ by employing interior point methods involving the worst case polynomial complexity of $\mathcal{O}\{\max(T, M)^4 M^{(1/2)} \log(1/\zeta)\}$ [53]. It is apparent from (22) and (23) that the order of the TDL implementation scheme is NL , whereas the DFT approach involves L unknown variables, each of order N . Therefore, the polynomial complexity for TDL implementation scheme is $\mathcal{O}\{(NL)^{4.5} \log(1/\zeta)\}$, and is $\mathcal{O}\{N^{4.5} \log(1/\zeta)\}$ (assuming $N > L$) for the DFT implementation scheme. This renders the latter computationally viable. The polynomial complexity of SCA for TDL implementation scheme is $\mathcal{O}\{(NL)^3 \log(1/\zeta)\}$, and is $\mathcal{O}\{N^3 \log(1/\zeta)\}$ for the DFT implementation. Hence, polynomial complexity is considerably lower for SCA as compared to the SDR formulation, as the latter intrinsically squares the number of variables involved, essentially exacerbating the runtime [45].

IV. SPARSE MATRIX COMPLETION OF BLOCK TOEPLITZ MATRICES

The aforementioned sparse array design formulations require the received data correlation matrix corresponding to the full array aperture. This is a rather stringent requirement in an adaptive switching environment where the data is fetched from only P active sensor locations over a given observation period. The received data correlation matrix for the sparse array design using TDL implementation scheme has $L^2(N^2 - P^2)$ missing

correlation entries, whereas there are $L(N^2 - P^2)$ missing correlation values for the DFT implementation scheme. Clearly, for the large values of L , the TDL implementation scheme has significantly higher number of missing correlation entries as compared to the DFT implementation scheme.

Recently, the hybrid sparse design for the narrowband beamforming was introduced to alleviate the issue of missing correlation lags in the received data correlation matrix [54]. This is primarily achieved by pre-allocating few sensors to guarantee a fully augmentable sparse array, while engaging the remaining degrees of freedom (DOF) to maximize the SINR. However, locking in few DOFs to ensure the array full augmentability can lead to suboptimal sparse beamformers. Alternatively, the matrix completion approach can be used to provide the missing lags [55]–[57]. We propose, herein, sparse matrix completion to efficiently exploit the structure of the data correlation matrix to recover the missing correlation values. The received data correlation matrix for the TDL implementation scheme is a Hermitian positive definite matrix but it also follows a block Toeplitz formation, as shown below,

$$\mathbf{R} = \begin{bmatrix} \mathbb{T}_0 & \mathbb{T}_1 & \mathbb{T}_2 & \dots & \mathbb{T}_{L-1} \\ \mathbb{T}_{-1} & \mathbb{T}_0 & \mathbb{T}_1 & \dots & \mathbb{T}_{L-2} \\ \mathbb{T}_{-2} & \mathbb{T}_{-1} & \mathbb{T}_0 & \dots & \mathbb{T}_{L-3} \\ \vdots & \vdots & \vdots & \ddots & \vdots \\ \mathbb{T}_{-(L-1)} & \mathbb{T}_{-(L-2)} & \mathbb{T}_{-(L-3)} & \dots & \mathbb{T}_0 \end{bmatrix} \quad (33)$$

By definition, block Toeplitz matrices doesn't necessitate each comprising block to be Toeplitz within itself. Therefore, matrix \mathbf{R} in (33) represents a special case of block Toeplitz matrices, where the Toeplitz structure is also preserved for each constituent block $\mathbb{T}_k \in \mathbb{C}^{N \times N}$. Because of the matrix Hermitian symmetry, we also have $\mathbb{T}_k^H = \mathbb{T}_{-k}$ (for $k \neq 0$). Instead of recovering \mathbf{R} as a single unit, we focus on completing the constituent blocks and then synthesizing the full correlation matrix \mathbf{R} . This approach potentially caps the computational expenses considerably but also efficiently exploits the formation of \mathbf{R} .

There is an important distinction between the constituent blocks \mathbb{T}_0 and \mathbb{T}_k (for $k \neq 0$). It is noted that \mathbb{T}_0 is positive definite Hermitian Toeplitz matrix, whereas \mathbb{T}_k (for $k \neq 0$) are indefinite Toeplitz matrices which are not necessarily Hermitian. Therefore, we resort to two different ways with regards to our treatment of \mathbb{T}_0 and \mathbb{T}_k while adopting a Toeplitz matrix completion scheme under the low rank assumption. It is known that the correlation matrix \mathbf{R} for the wideband far field sources impinging on the ULA resultantly follows the structure in (33) and can be represented effectively with a relatively low rank approximation depending on the observed source time-bandwidth product [14]. The trace heuristic is a well known approach which is adopted generally as a convex surrogate in recovering low rank matrices. This approach has been successfully used in many areas of control systems and array processing to recover simpler and low rank data models [53],

[58], [59]. Moreover, it has been shown that the trace heuristic is equivalent to the nuclear norm minimization in recovering positive semidefinite correlation matrices [57], [60]–[62]. The low rank positive semidefinite Toeplitz matrix completion problem has been proposed in [63] for interpolating missing correlation lags in coprime array configuration and can be adopted to interpolate \mathbb{T}_0 as follows,

$$\begin{aligned} & \underset{l \in \mathbb{C}^N}{\text{minimize}} \quad \|\mathcal{T}(l) \odot \mathbf{Z} - \overset{\circ}{\mathbb{T}}_0\|_F^2 + \zeta \text{Tr}(\mathcal{T}(l)) \\ & \text{s.t.} \quad \mathcal{T}(l) \succeq 0 \end{aligned} \quad (34)$$

Here, the unknown Hermitian Toeplitz matrix $\mathcal{T}(l)$, can uniquely be defined by a single vector l representing the first row of $\mathcal{T}(l)$, and l^H denoting the matrix first column. Matrix $\overset{\circ}{\mathbb{T}}_0$ is the received data correlation matrix with the missing correlation values set equal to zero. The element wise product is denoted by symbol ' \odot ' and ' \succeq ' implements the positive semidefinite constraint. The objective function attempts to minimize the error between the observed correlation values and the corresponding entries of $\mathcal{T}(l)$ implemented through the Frobenius norm of the error matrix (The function ' $\|\cdot\|_F^2$ ', represents the square of the Frobenius norm of matrix which returns the sum of square of it's entries). The parameter ' ζ ' pursues the trade off between the denoising term and the trace heuristic to recover a simpler low rank model. The nominal value of the parameter ' ζ ' is challenging to locate and is typically gleaned from the numerical experience. In order to do away with the nuisance parameter ' ζ ', we adopt a fusion based approach more suited to our application. We note that the non zero elements in $\overset{\circ}{\mathbb{T}}_0$ can be segregated into two classes. With regards to the sparse entries in $\overset{\circ}{\mathbb{T}}_0$, either we have the whole sub-diagonal entries missing in $\overset{\circ}{\mathbb{T}}_0$ or the sub-diagonals are sparse. The former situation arises if there is missing correlation lag in $\overset{\circ}{\mathbb{T}}_0$, whereas the latter arises when the corresponding correlation lag is present but lacking the intrinsic redundancy corresponding to the compact sensor grid. The observed correlation lags are averaged across the sub diagonal to filter the sensor noise as follows,

$$\hat{l}^i(k) = \left(\frac{1}{c_k}\right) \sum_{\forall m-n=k} \overset{\circ}{\mathbb{T}}_0^i(m, n) \quad (35)$$

Here, $\overset{\circ}{\mathbb{T}}_0^i$ is the $\mathbf{R}(i, i)$ entry in (33) denoting the estimate of $\overset{\circ}{\mathbb{T}}_0$ at i th sampling instance, $k \in 0, 1, \dots, N-1$ represents the respective lag or the sub diagonal of $\overset{\circ}{\mathbb{T}}_0$ and c_k is the observed redundancy of the k th lag. As evident in (33), there are L copies of $\overset{\circ}{\mathbb{T}}_0$ corresponding to L sampling instances. Hence, $\hat{l}^i(k)$ is averaged over L blocks to yield an estimate of the given lag $\hat{l}(k) = \frac{1}{L} \sum_{i=0}^{L-1} \hat{l}^i(k)$. The fused matrix completion formulation, therefore, substitutes the sparse sub-diagonals with the estimated average value $\hat{l}(k)$, whereas the

completely missing sub-diagonals are interpolated as follows,

$$\begin{aligned} & \underset{l \in \mathbb{C}^N}{\text{minimize}} \quad \text{Tr}(\mathcal{T}(l)) \\ & \text{s.t.} \quad l(\text{lag present}) = \hat{l}(k), \\ & \quad \quad \mathcal{T}(l) \succeq 0 \end{aligned} \quad (36)$$

The above formulation relies on fairly accurate estimate of the observed correlation lag which not only involves averaging over the corresponding sub diagonal but also across L sampling instances. Such accuracy can become challenging to meet the semidefinite constraint if the available degrees of freedom are few. To circumvent this problem, the 0 lag is removed from the constraint which gives the additional degree of freedom to the algorithm to set aside an appropriate loading factor to make the problem feasible. It is noted that the formulation in (36) would choose the minimum possible diagonal loading as it requires to minimize the trace heuristic and hence strives to maximize the sparse eigenvalues.

The trace heuristic can also be extended for indefinite matrices to recover sparse models [64]. We couple this observation along with the above discussion to perform low rank matrix completion for \mathbb{T}_k (for $k \neq 0$) as follows,

$$\begin{aligned} & \underset{l_r, l_c \in \mathbb{C}^N}{\text{minimize}} \quad \text{Tr}(\mathbf{W}_1) + \text{Tr}(\mathbf{W}_2) \\ & \text{s.t.} \quad l_r(\text{lag present}) = \hat{l}_r(k), \\ & \quad \quad l_c(\text{lag present}) = \hat{l}_c(k), \\ & \quad \quad \begin{bmatrix} \mathbf{W}_1 & \mathcal{T}(l_r, l_c) \\ \mathcal{T}(l_r, l_c) & \mathbf{W}_2 \end{bmatrix} \succeq 0 \end{aligned} \quad (37)$$

Here, \mathbf{W}_1 and \mathbf{W}_2 are auxiliary matrices implementing trace heuristic to recover low rank indefinite matrices. The function $\mathcal{T}(l_r, l_c)$ returns the Toeplitz matrix with l_r and l_c being the first row and the first column, respectively. This distinction is important as in general \mathbb{T}_k (for $k \neq 0$) is not a Hermitian Toeplitz matrix. The formulation in (37) is repeated to yield an estimate for all constituent Toeplitz blocks.

Upon performing matrix completion for each constituent Toeplitz block, the individual Toeplitz blocks can be plugged back into (33) to yield an estimate $\hat{\mathbf{R}}$. We can improve the estimate $\hat{\mathbf{R}}$ by incorporating the noise variance which is generally known or estimated apriori. This is achieved through the maximum likelihood estimate (MLE) approach where the eigenvalues corresponding to the eigenvectors of the noise subspace are set equal to the noise floor while the remaining eigenvalues are kept the same. The MLE of $\hat{\mathbf{R}}$ is denoted by $\hat{\mathbf{R}}$ and is given by the outer product of the original eigenvectors of $\hat{\mathbf{R}}$ reweighted by the modified eigenvalues. However, it is noted that in practice the number of eigenvectors associated with the noise floor are not exactly known. Nevertheless, we only reset those eigenvalues which are less than the noise floor. Finally, the maximum likelihood estimate $\hat{\mathbf{R}}$, is used in lieu of $\hat{\mathbf{R}}$, to carry out the data dependent optimization for MaxSINR. It is also noted that unlike $\hat{\mathbf{R}}$, the matrix $\hat{\mathbf{R}}$ is no longer block Toeplitz but is now guaranteed to be positive definite as is strictly required to implement the proposed sparse optimization algorithms. The formulation in (36) is sufficient for the DFT implementation scheme which only involves L received data matrices corresponding to the L DFT bins.

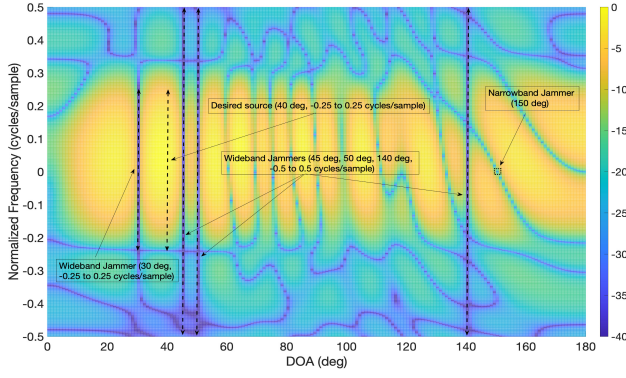


Fig. 4: Frequency dependent beampattern for the array configuration recovered through convex relaxation.

V. SIMULATIONS

The effectiveness of the sparse array design for MaxSINR beamforming is demonstrated by design examples considering a wideband source operating in the presence of a mix of narrowband and wideband jammers. The MATLAB-based CVX modeling tool is used for convex optimization. The importance of sparse array design for MaxSINR is further emphasized by comparing the optimum design with the sub optimum array configurations under the TDL and DFT implementation schemes. The simulation results are presented for perspective linear sensor locations, nevertheless, the proposed algorithms are applicable to rectangular grid points or arbitrary placed sensors on 3D surfaces.

A. Example 1

The task is to select $P = 8$ sensors from $N = 20$ possible equally spaced locations with inter-element spacing of $\lambda_{min}/2$. We consider 8 delay line filter taps associated with each selected sensor (8 DFT bins for DFT implementation scheme) implying $L = 8$. A desired wideband point source impinges on a linear array from DOA 40° . The fractional bandwidth of the system w.r.t. the center frequency is 0.22. The desired source has uniform PSD (power spectral density), occupying the normalized frequency spectrum from -0.25 to 0.25 cycles/sample. Three strong wideband jammers occupying the entire frequency band from -0.5 to 0.5 cycles/sample, are located at angles 45° , 50° and 140° . There is another wideband jammer at 30° , covering the same spectrum as that of the desired source (-0.25 to 0.25 cycles/sample). In addition, a narrowband jammer lock onto the source carrier frequency is located at 150° . The SNR of the desired signal is 0 dB, and the INR of each interfering signals is set to 30 dB.

Figure 4 shows the frequency dependent beampattern for the array configuration recovered through TDL-SDR. It is evident from the beampattern that a high gain is maintained throughout the band of interest for the desired source signal while alleviating the interferers from respective DOAs and frequency bands. These beampattern characteristics translate to an output SINR of 8.96 dB. The TDL-SDR performs close to the optimum array found by enumeration which has an output

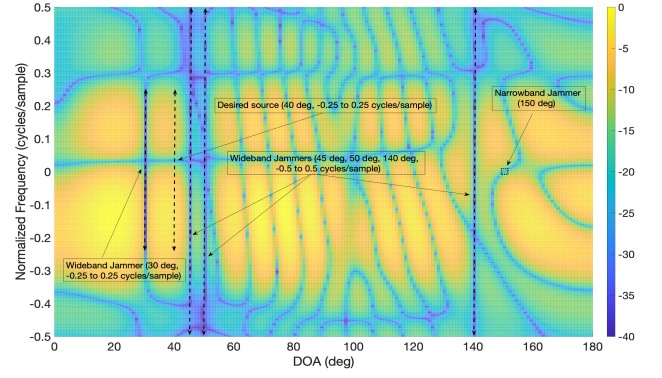


Fig. 5: Frequency dependent beampattern for the array configuration shown in Fig. 6f.

SINR of 9.3 dB. The corresponding sparse array configurations obtained by enumeration and TDL-SDR are shown in the Fig. 6a and 6b, respectively (the green color denotes the sensor locations selected, whereas the gray color shows the sensor locations not selected). It is important to mention that the optimum array found by enumeration requires a search over 125970 possible sparse array configurations, which has a prohibitive computational cost attributed to expensive singular value decomposition (SVD) for each enumeration. The optimum sparse array design achieved through TDL-SCA is shown in Fig. 6c. This array configuration is capable of delivering output SINR of 6.81 dB with the use of optimal beamforming weights. This performance is inferior to that of the sparse array found through TDL-SDR by around 2 dB, however with less computational complexity.

In general, for any given array configuration, the TDL implementation scheme yields marginally higher SINR as compared to the DFT implementation scheme. Owing to the reduced computational cost of the DFT sparse design, and relatively better performance of the TDL sparse design, one can entwine TDL and DFT beamformers to capitalize on the merits of both approaches. That is, we proceed to find the optimum TDL beamformer weights based on the sensor array configuration that results from the optimum DFT-based implementation scheme. This refer a dual-domain design implementation scheme since it considers both time and frequency domains in generating the optimum receiver design. This design has slightly elevated computational expense over the DFT design, as it involves calculating the optimum TDL beamformer weights corresponding to the DFT optimized configuration. For the underlying problem, the dual-domain design, through the DFT-SDR and DFT-SCA gives an output SINR of 8 dB and 8.8 dB respectively, which is close to the maximum possible SINR of 9.3 dB. The sparse array configurations rendered by DFT-SDR and DFT-SCA are shown in Figs. 6d and 6e. Therefore, we remark that for the example considered, the dual domain design underlying the DFT implementation scheme, performs closely to the design carried out exclusively by the TDL implementation scheme.

Sparse array design utilizes the array aperture and the additional degrees of freedom, made available by the switching

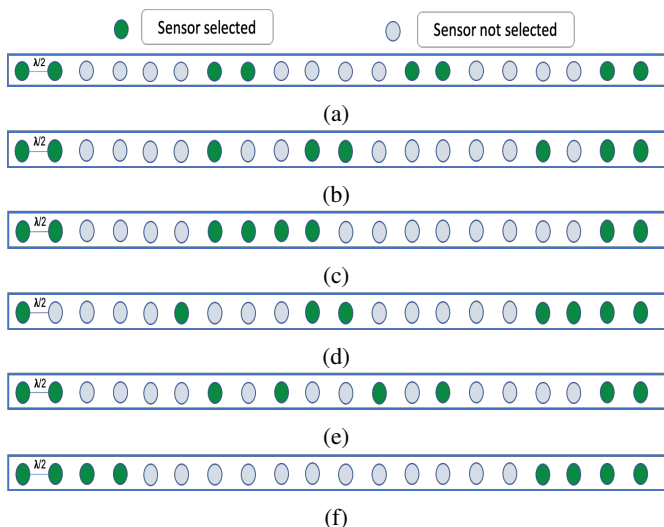


Fig. 6: Example 1 - (a) Optimum array TDL implementation scheme (Enumeration) (b) TDL-SDR (c) TDL-SCA (d) DFT-SDR (e) DFT-SCA (f) 8 sensor centrally sparse array

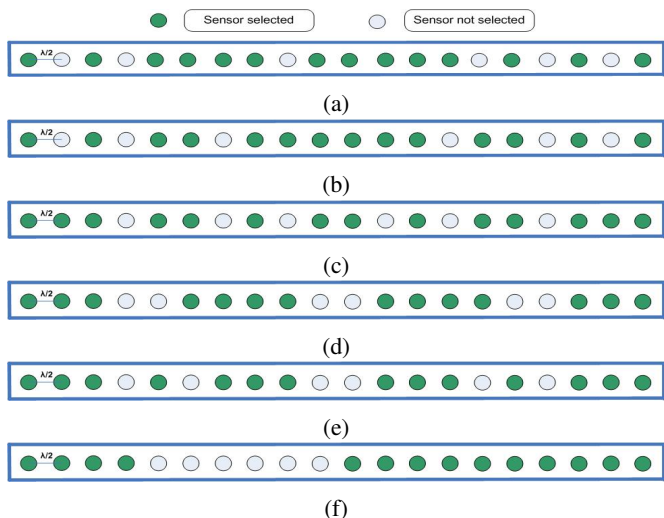


Fig. 7: Example 2 - (a) Optimum array TDL implementation scheme (Enumeration) (b) TDL-SCA (c) TDL-SDR (d) DFT-SCA (e) DFT-SDR (f) Worst case array (TDL, DFT)

transceiver chains, to yield considerable SINR improvement. To demonstrate such improvement, the sparse array configuration, shown in Fig. 6f, is selected which occupies the entire array aperture. It can be observed from the beampattern of this array, shown in Fig. 5, that, in an effort to remove the strong interfering signals, the sparse array failed to provide maximum gain towards the source of interest. This results in a considerable low output SINR of 0.8 dB. The actual run times for the SDR-TDL and SDR-DFT approaches are around 16s and 5s per iteration, respectively (1.4 GHz Quad-Core Intel i5 processor), whereas it is around 1s for the SCA-TDL and SCA-DFT approaches.

B. Example 2

Consider a wideband source of interest at 45^0 and the wideband jammers located at 35^0 , 55^0 , 60^0 , 145^0 and 155^0 . A narrowband jammer is located at 135^0 at an operating frequency of f_c , all other parameters are the same as in Example 1 except that $P = 14$ sensor locations selected from $N = 20$ possible locations and the wideband source and jammers occupy the entire spectrum from -0.5 to 0.5 cycles/sample. The SINR of the optimum array for the TDL implementation scheme (Fig. 7a) is 11.32 dB (found through enumeration). Optimization performed using SCA yields the array in Fig. 7b, with respective SINR of 11.2 dB, whereas that performed by SDR yields the array shown in Fig. 7c and corresponding SINR of 10.9 dB. For the dual domain design, the optimum sparse arrays found through DFT-SCA (Fig. 7d) and through the DFT-SDR algorithm (Fig. 7e) deliver an approximately similar output SINR, around 11.02 dB. This is inferior to the exclusive TDL design. It is important to note that the array configuration resulting in the worst case performance, shown in Fig. 7f, spans the full aperture as the optimum array, yet it offers an output SINR of only 7.35 dB, underscoring the importance of carefully performing sensor selection for the sparse array design.

C. Comparison of SDR and SCA under both models

The design examples discussed thus far show amicable performance of the proposed algorithms under the assumption of the knowledge of full data correlation matrix. The results clearly tie the performance to the location of the sources and their respective powers. However, evaluating the performance under matrix completion involves analysis for additional variables, namely, the initial sparse array configuration prior to optimization and the number of snapshots. The performance is, therefore, dependent on the observed realization of the received data. In order to have a holistic assessment of the proposed algorithms, Monte Carlo simulations are generated. We select $P = 8$ locations out of $N = 16$ available locations. For specified DOA of the desired source, trials are generated involving six jammers occupying random locations from 30^0 to 150^0 . The SNR of the desired source is 0 dB, while the powers of the jammers are uniformly distributed from 10 to 20 dB. The simulation is repeated at 11 different desired source DOAs, and the average SINR computed. In total, 1500 experiments are conducted. For each trial, a random P -sparse array topology serves as an initial array configuration. This configuration could be an optimized configuration from the preceding operating conditions. The sparse data correlation matrix is estimated based on sensor locations in the initial configuration before performing matrix completion and subsequent optimization process. The binary search for the sparsity parameter μ ranges from 0.01 to 3, sparsity threshold $\gamma = 10^{-3}$ and $\epsilon = 0.05$, relative signal bandwidths and other parameters are the same as given in Example 1.

Three benchmarks are established to access the performance of the proposed algorithm under limited snapshots and lack of knowledge of the full data correlation matrix. The first benchmark applies the enumeration technique for MaxSINR

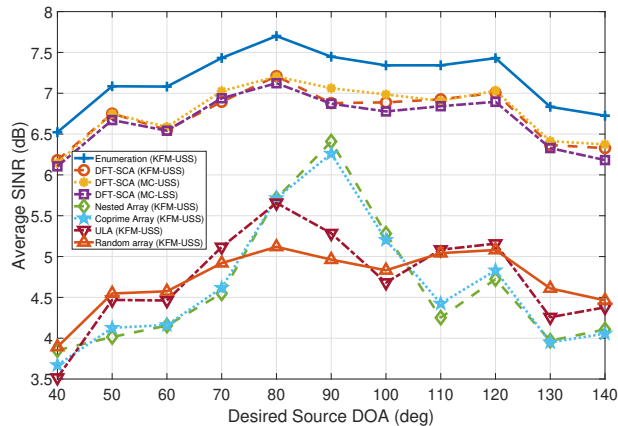


Fig. 8: Performance comparisons of SCA under DFT model.

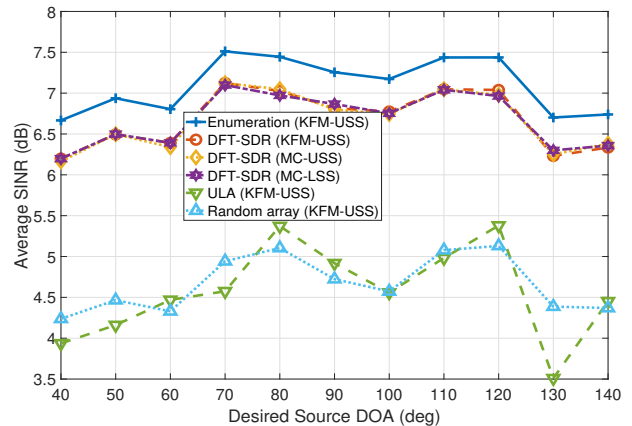


Fig. 10: Performance comparisons of SDR under DFT model.

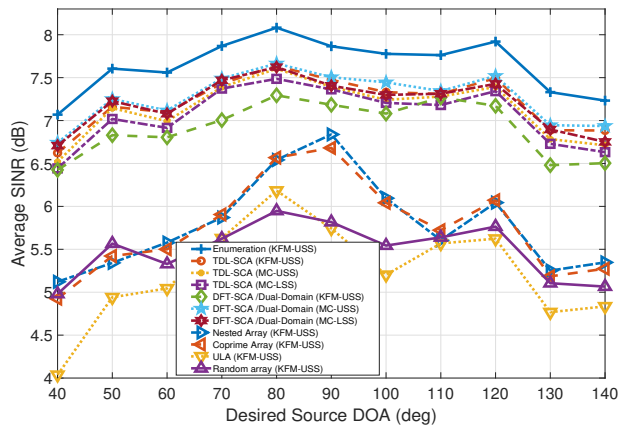


Fig. 9: Performance comparisons of SCA under TDL model.

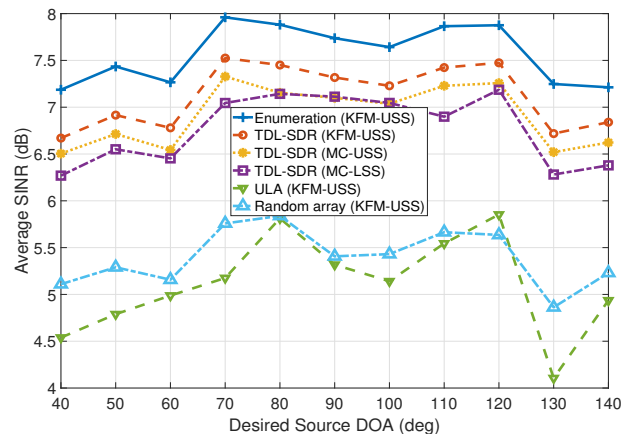


Fig. 11: Performance comparisons of SDR under TDL model.

design under the assumption that the data from all the perspective sensor locations is available and accurate knowledge of the data correlation matrix, i.e., assuming unlimited number of snapshots. This benchmark is referred to as “Knowledge of Full Correlation Matrix-Unlimited Snapshots (KFM-USS)”. Other benchmarks utilize matrix completion to recover the missing lags (corresponding to $N - P$ missing sensors). We refer to these benchmarks as “Matrix Completion-Unlimited Snapshots (MC-USS)” and “Matrix Completion-Limited Snap Shots (MC-LSS),” depending on whether the correlation values are accurately known through unlimited snapshots or estimated from the limited snapshots. The evaluation under limited snapshots considers $T = 500$.

The performance of the SCA algorithm for the DFT implementation scheme is shown in the Fig. 8. The performance upper bound is given by the MaxSINR design evaluated through enumeration (DFT-Enumeration (KFM-USS)). In this case, the average performance over all the desired source DOAs is 7.24 dB. The proposed DFT-SCA algorithm under the KFM-USS benchmark offers an average SINR of 6.63 dB. This performance is also comparable to the one achieved through the proposed matrix completion, as is evident in Fig. 8. However, the DFT-SCA design incorporating the MC-

LSS benchmark ($T = 500$) has a slight performance trade off of 0.14 dB w.r.t. the DFT-SCA MC-USS design. The aforementioned robustness of the MaxSINR design under limited snapshots is partially attributable to a rather accurate full matrix estimate achieved by incorporating the a priori knowledge of noise floor.

The performance of the SCA under the TDL model is evaluated based on the aforementioned benchmarks, as depicted in Fig. 9. The performance trends are similar, however, the average SINR offered by the TDL implementation scheme is slightly superior to the DFT implementation scheme which is consistent with the literature on wideband beamforming for compact arrays [15]. Moreover, it is noted that the DFT-SCA dual domain design achieves comparable performance to the TDL-SCA under all design benchmarks. This demonstrates the potential of the dual design in achieving an effective MaxSINR beamformer with reduced complexity. Figs. 10 and 11 depict the Monte Carlo performance results analyzing the proposed SDR. It shows that the SDR offers comparable performance to the SCA technique, but involves a heavy computational overhead. It is also clear from the plots that the optimized array configurations offer a consequential advantage over both the compact ULA and the high resolution structured arrays, such

as coprime and nested arrays [16], [18], and the randomly selected P sparse array configuration, each employing their respective optimal beamforming weights. The average worst case SINR is, however, reduced significantly to only 1.1 dB. The performance is also re-evaluated at varying number of snapshots with consistent results. The performances of the proposed algorithms under MC-LSS inch closer to the MC-USS benchmark with increased data.

D. Practical Considerations for sparse array design

To assess the SINR advantage of the optimum sparse array design, we consider the effect of two important environment dependent parameters, namely, the DOA of the desired source and the relative locations of the jammers w.r.t. the desired source. To demonstrate this effect, the desired source DOA in the above examples is changed in steps of 5° , with the relative locations of the jammers remaining the same with respect to the desired source. For example, when the desired source is at 50° instead of 45° , the corresponding jammer locations shift by 5° . Figure 12 compares the performance of the optimal configuration, the worst performing array, and the compact ULA, with the desired source DOA varying from 30° to 60° under Example 2 and modified Example 2 scenario. In the modified Example 2, all the parameters are kept the same except the desired source is assumed at 40° instead of 45° . It is evident from Fig. 12 that under all scenarios generated under modified Example 2, the compact ULA delivers the worst performance, irrespective of the desired source DOA. This is because the jammers are located closer to the source of interest and the compact ULA lacks the resolution due to its limited array aperture. On the other hand, for Example 2, the jammers are comparatively widely spaced and as such, the compact ULA has a satisfactory performance that is close to the optimum sparse arrays, especially when the source DOAs are near the array broadside. The performance degradation of the ULA near end-fire is due to the increasing overlap between the desired signal subspace and the interference plus noise subspace [65], therefore lowering SINR performance. In such scenarios, the sparse array design efficiently utilizes its degrees of freedom to improve SINR by increasing the separation between the two subspaces. These examples show that the sparse array design is most critical when the underlying jamming environment calls for additional degrees of freedom to engage the available array aperture more efficiently and to fulfill the resolution requirements posed by the closer proximity of jammers and the desired source DOA.

VI. CONCLUSION

This paper considered optimum sparse array design for maximizing the beamformer output SINR for the case of wideband signal models. Two different implementations, namely the TDL and the DFT implementation schemes, were presented for the optimum sparse array design. The DFT implementation scheme reduces the MaxSINR sparse array design problem to the lower dimensional space, thereby reducing computational cost. The sparse array configuration optimized in the DFT domain and later imported to the TDL implementation

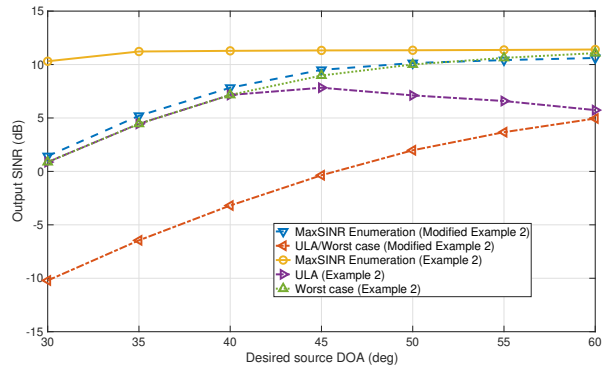


Fig. 12: Performance comparisons of the optimum sparse array, the worst performing array and the compact ULA (TDL implementation scheme).

scheme is analyzed to alleviate the computational cost of the TDL sparse implementation. It was shown that the imported design can possibly yield comparable performance to the design carried out exclusively through the TDL implementation scheme. For both approaches, we solved the problem using the iterative unit rank promoting SDR algorithm and a simplified implementation using SCA. The parameter-free block Toeplitz matrix completion was proposed to realize the data dependent design. It was shown that the SDR and SCA formulation perform reasonably close to the optimum sparse array design achieved through enumeration under limited data snapshots. The MaxSINR optimum sparse array yielded considerable performance improvement over suboptimal sparse arrays and compact ULA for the underlying sensing scenarios.

REFERENCES

- [1] S. A. Hamza and M. G. Amin, "Optimum sparse array receive beamforming for wideband signal model," in *2018 52nd Asilomar Conference on Signals, Systems, and Computers*, Oct 2018, pp. 89–93.
- [2] —, "Sparse array DFT beamformers for wideband sources," *2019 IEEE Radar Conference (RadarConf)*, Apr 2019. [Online]. Available: <http://dx.doi.org/10.1109/RADAR.2019.8835749>
- [3] L. Yang and G. B. Giannakis, "Ultra-wideband communications: an idea whose time has come," *IEEE Signal Processing Magazine*, vol. 21, no. 6, pp. 26–54, Nov 2004.
- [4] M. S. Brandstein and D. B. Ward, "Microphone arrays - signal processing techniques and applications," in *Microphone Arrays*, 2001.
- [5] A. Goldsmith, *Wireless Communications*. New York, NY, USA: Cambridge University Press, 2005.
- [6] C. Paulson, J. Chang, C. Romero, J. Watson, F. Pearce, and N. Levin, "Ultra-wideband radar methods and techniques of medical sensing and imaging," in *Proceedings of SPIE - The International Society for Optical Engineering*, B. Cullum and J. Carter, Eds., vol. 6007, 2005.
- [7] E. Pancera, "Medical applications of the ultra wideband technology," in *2010 Loughborough Antennas Propagation Conference*, Nov 2010, pp. 52–56.
- [8] E. D. Di Claudio and R. Parisi, *Robust Wideband Beamforming*. John Wiley & Sons, Ltd, 2005, ch. 7, pp. 353–415.
- [9] W. Liu and S. Weiss, *Wideband beamforming: concepts and techniques*, ser. Wireless Communications and Mobile Computing. Wiley-Blackwell, Mar. 2010, ISBN: 978-0-470-71392-1.
- [10] K. Buckley, "Spatial/spectral filtering with linearly constrained minimum variance beamformers," *IEEE Transactions on Acoustics, Speech, and Signal Processing*, vol. 35, no. 3, pp. 249–266, March 1987.
- [11] B. D. V. Veen and K. M. Buckley, "Beamforming: a versatile approach to spatial filtering," *IEEE ASSP Magazine*, vol. 5, no. 2, pp. 4–24, April 1988.

- [12] O. L. Frost, "An algorithm for linearly constrained adaptive array processing," *Proceedings of the IEEE*, vol. 60, no. 8, pp. 926–935, Aug 1972.
- [13] M. Er and A. Cantoni, "Derivative constraints for broad-band element space antenna array processors," *IEEE Transactions on Acoustics, Speech, and Signal Processing*, vol. 31, no. 6, pp. 1378–1393, Dec 1983.
- [14] K. Buckley and L. Griffiths, "An adaptive generalized sidelobe canceller with derivative constraints," *IEEE Transactions on Antennas and Propagation*, vol. 34, no. 3, pp. 311–319, March 1986.
- [15] L. C. Godara, "Application of the fast fourier transform to broadband beamforming," *The Journal of the Acoustical Society of America*, vol. 98, no. 1, pp. 230–240, 1995. [Online]. Available: <https://doi.org/10.1121/1.413765>
- [16] P. Pal and P. P. Vaidyanathan, "Coprime sampling and the music algorithm," in *2011 Digital Signal Processing and Signal Processing Education Meeting (DSP/SPE)*, Jan. 2011, pp. 289–294.
- [17] S. Qin, Y. D. Zhang, and M. G. Amin, "Generalized coprime array configurations for direction-of-arrival estimation," *IEEE Transactions on Signal Processing*, vol. 63, no. 6, pp. 1377–1390, March 2015.
- [18] P. Pal and P. P. Vaidyanathan, "Nested arrays: A novel approach to array processing with enhanced degrees of freedom," *IEEE Transactions on Signal Processing*, vol. 58, no. 8, pp. 4167–4181, Aug. 2010.
- [19] E. BouDaher, Y. Jia, F. Ahmad, and M. G. Amin, "Multi-frequency coprime arrays for high-resolution direction-of-arrival estimation," *IEEE Transactions on Signal Processing*, vol. 63, no. 14, pp. 3797–3808, July 2015.
- [20] J. Sheinvald and M. Wax, "Direction finding with fewer receivers via time-varying preprocessing," *IEEE Transactions on Signal Processing*, vol. 47, no. 1, pp. 2–9, Jan 1999.
- [21] Moon-Sik Lee, V. Katkovnik, and Yong-Hoon Kim, "System modeling and signal processing for a switch antenna array radar," *IEEE Transactions on Signal Processing*, vol. 52, no. 6, pp. 1513–1523, June 2004.
- [22] Li Yang, Liang Liwan, Pan Weifeng, Chen Yaqin, and Feng Zhenghe, "Signal processing method for switch antenna array of the fmcw radar," in *Proceedings of the 2001 IEEE Radar Conference (Cat. No.01CH37200)*, May 2001, pp. 289–293.
- [23] Y. Asano, S. Ohshima, T. Harada, M. Ogawa, and K. Nishikawa, "Proposal of millimeter-wave holographic radar with antenna switching," in *2001 IEEE MTT-S International Microwave Symposium Digest (Cat. No.01CH37157)*, vol. 2, May 2001, pp. 1111–1114 vol.2.
- [24] M. Guo, Y. D. Zhang, and T. Chen, "DOA estimation using compressed sparse array," *IEEE Transactions on Signal Processing*, vol. 66, no. 15, pp. 4133–4146, Aug 2018.
- [25] X. Wang, E. Aboutanios, M. Trinkle, and M. G. Amin, "Reconfigurable adaptive array beamforming by antenna selection," *IEEE Transactions on Signal Processing*, vol. 62, no. 9, pp. 2385–2396, May 2014.
- [26] X. Wang, M. Amin, X. Wang, and X. Cao, "Sparse array quiescent beamformer design combining adaptive and deterministic constraints," *IEEE Transactions on Antennas and Propagation*, vol. 65, no. 11, pp. 5808–5818, Nov 2017.
- [27] X. Wang, M. Amin, and X. Cao, "Analysis and design of optimum sparse array configurations for adaptive beamforming," *IEEE Transactions on Signal Processing*, vol. 66, no. 2, pp. 340–351, Jan 2018.
- [28] X. Wang, M. G. Amin, and X. Wang, "Optimum sparse array design for multiple beamformers with common receiver," in *2018 IEEE International Conference on Acoustics, Speech and Signal Processing*, 2018.
- [29] O. Mehanna, N. D. Sidiropoulos, and G. B. Giannakis, "Joint multicast beamforming and antenna selection," *IEEE Transactions on Signal Processing*, vol. 61, no. 10, pp. 2660–2674, May 2013.
- [30] N. D. Sidiropoulos, T. N. Davidson, and Z.-Q. Luo, "Transmit beamforming for physical-layer multicasting," *IEEE Transactions on Signal Processing*, vol. 54, no. 6, pp. 2239–2251, June 2006.
- [31] W. Roberts, L. Xu, J. Li, and P. Stoica, "Sparse antenna array design for MIMO active sensing applications," *IEEE Transactions on Antennas and Propagation*, vol. 59, no. 3, pp. 846–858, March 2011.
- [32] M. H. Bae, I. H. Sohn, and S. B. Park, "Grating lobe reduction in ultrasonic synthetic focusing," *Electronics Letters*, vol. 27, no. 14, pp. 1225–1227, July 1991.
- [33] J. Lu and J. Greenleaf, "Study of two-dimensional array transducers for limited diffraction beams," *IEEE Transactions on Ultrasonics, Ferroelectrics, and Frequency Control*, vol. 41, no. 5, pp. 724–739, 9 1994.
- [34] J. H. Doles and F. D. Benedict, "Broad-band array design using the asymptotic theory of unequally spaced arrays," *IEEE Transactions on Antennas and Propagation*, vol. 36, no. 1, pp. 27–33, Jan 1988.
- [35] V. Murino, A. Trucco, and A. Tesei, "Beam pattern formulation and analysis for wide-band beamforming systems using sparse arrays," *Signal Processing*, vol. 56, no. 2, pp. 177 – 183, 1997.
- [36] V. Murino, A. Trucco, and C. S. Regazzoni, "Synthesis of unequally spaced arrays by simulated annealing," *IEEE Transactions on Signal Processing*, vol. 44, no. 1, pp. 119–122, Jan 1996.
- [37] D. B. Ward, R. A. Kennedy, and R. C. Williamson, "Theory and design of broadband sensor arrays with frequency invariant far-field beam patterns," *The Journal of the Acoustical Society of America*, vol. 97, no. 2, pp. 1023–1034, 1995.
- [38] A. Trucco, "Synthesizing wide-band sparse arrays by simulated annealing," in *MTS/IEEE Oceans 2001. An Ocean Odyssey. Conference Proceedings (IEEE Cat. No.01CH37295)*, vol. 2, Nov 2001, pp. 989–994 vol.2.
- [39] F. Anderson, W. Christensen, L. Fullerton, and B. Kortegaard, "Ultra-wideband beamforming in sparse arrays," *IEE Proceedings H - Microwaves, Antennas and Propagation*, vol. 138, no. 4, pp. 342–346, Aug 1991.
- [40] M. B. Hawes and W. Liu, "Sparse array design for wideband beamforming with reduced complexity in tapped delay-lines," *IEEE/ACM Transactions on Audio, Speech, and Language Processing*, vol. 22, no. 8, pp. 1236–1247, Aug 2014.
- [41] I. S. Reed, J. D. Mallett, and L. E. Brennan, "Rapid convergence rate in adaptive arrays," *IEEE Transactions on Aerospace and Electronic Systems*, vol. AES-10, no. 6, pp. 853–863, Nov. 1974.
- [42] H. L. V. Trees, *Detection, Estimation, and Modulation Theory: Radar-Sonar Signal Processing and Gaussian Signals in Noise*. Melbourne, FL, USA: Krieger Publishing Co., Inc., 1992.
- [43] J. Li, P. Stoica, and Z. Wang, "On robust capon beamforming and diagonal loading," *IEEE Transactions on Signal Processing*, vol. 51, no. 7, pp. 1702–1715, July 2003.
- [44] S. Shahbazpanahi, A. B. Gershman, Z.-Q. Luo, and K. M. Wong, "Robust adaptive beamforming for general-rank signal models," *IEEE Transactions on Signal Processing*, vol. 51, no. 9, pp. 2257–2269, Sept. 2003.
- [45] M. S. Ibrahim, A. Konar, M. Hong, and N. D. Sidiropoulos, "Mirrorprox sca algorithm for multicast beamforming and antenna selection," *2018 IEEE 19th International Workshop on Signal Processing Advances in Wireless Communications (SPAWC)*, pp. 1–5, 2018.
- [46] M. G. Amin, P. P. Vaidyanathan, Y. D. Zhang, and P. Pal, "Editorial for coprime special issue," *Digital Signal Processing*, vol. 61, no. Supplement C, pp. 1 – 2, 2017, special Issue on Coprime Sampling and Arrays.
- [47] S. A. Hamza and M. G. Amin, "Sparse array design for maximizing the signal-to-interference-plus-noise-ratio by matrix completion," *Digital Signal Processing*, p. 102678, 2020. [Online]. Available: <http://www.sciencedirect.com/science/article/pii/S1051200420300233>
- [48] S. A. Hamza and M. G. Amin, "Hybrid sparse array design for under-determined models," in *ICASSP 2019 - 2019 IEEE International Conference on Acoustics, Speech and Signal Processing (ICASSP)*, May 2019, pp. 4180–4184.
- [49] B. Fuchs, "Application of convex relaxation to array synthesis problems," *IEEE Transactions on Antennas and Propagation*, vol. 62, no. 2, pp. 634–640, Feb. 2014.
- [50] S. Eng Nai, W. Ser, Z. Liang Yu, and H. Chen, "Beampattern synthesis for linear and planar arrays with antenna selection by convex optimization," vol. 58, pp. 3923 – 3930, 01 2011.
- [51] E. J. Candès, M. B. Wakin, and S. P. Boyd, "Enhancing sparsity by reweighted l_1 minimization," *Journal of Fourier Analysis and Applications*, vol. 14, no. 5, pp. 877–905, Dec. 2008.
- [52] M. Bengtsson and B. Ottersten, "Optimal downlink beamforming using semidefinite optimization," 1999.
- [53] Z. q. Luo, W. k. Ma, A. M. c. So, Y. Ye, and S. Zhang, "Semidefinite relaxation of quadratic optimization problems," *IEEE Signal Processing Magazine*, vol. 27, no. 3, pp. 20–34, May 2010.
- [54] S. A. Hamza and M. G. Amin, "Hybrid sparse array beamforming design for general rank signal models," *IEEE Transactions on Signal Processing*, vol. 67, no. 24, pp. 6215–6226, Dec 2019.
- [55] Y. Abramovich, N. Spencer, and A. Gorokhov, "Positive-definite Toeplitz completion in DOA estimation for nonuniform linear antenna arrays. II. Partially augmentable arrays," *Trans. Sig. Proc.*, vol. 47, no. 6, pp. 1502–1521, Jun. 1999.
- [56] Y. I. Abramovich, D. A. Gray, A. Y. Gorokhov, and N. K. Spencer, "Positive-definite Toeplitz completion in DOA estimation for nonuniform linear antenna arrays. I. Fully augmentable arrays," *IEEE Transactions on Signal Processing*, vol. 46, no. 9, pp. 2458–2471, Sep 1998.
- [57] S. M. Hosseini and M. A. Sebt, "Array interpolation using covariance matrix completion of minimum-size virtual array," *IEEE Signal Processing Letters*, vol. 24, no. 7, pp. 1063–1067, July 2017.

- [58] B. Recht, M. Fazel, and P. A. Parrilo, "Guaranteed minimum-rank solutions of linear matrix equations via nuclear norm minimization," *SIAM Rev.*, vol. 52, no. 3, pp. 471–501, Aug. 2010.
- [59] K. Mohan and M. Fazel, "Iterative reweighted algorithms for matrix rank minimization," *J. Mach. Learn. Res.*, vol. 13, no. 1, pp. 3441–3473, Nov. 2012.
- [60] C. Zhou, Y. Gu, Z. Shi, and Y. D. Zhang, "Off-grid direction-of-arrival estimation using coprime array interpolation," *IEEE Signal Processing Letters*, vol. 25, no. 11, pp. 1710–1714, Nov 2018.
- [61] C. Liu, P. P. Vaidyanathan, and P. Pal, "Coprime coarray interpolation for DOA estimation via nuclear norm minimization," in *2016 IEEE International Symposium on Circuits and Systems (ISCAS)*, May 2016, pp. 2639–2642.
- [62] H. Qiao and P. Pal, "Gridless line spectrum estimation and low-rank Toeplitz matrix compression using structured samplers: A regularization-free approach," *IEEE Transactions on Signal Processing*, vol. 65, no. 9, pp. 2221–2236, May 2017.
- [63] C. Zhou, Y. Gu, X. Fan, Z. Shi, G. Mao, and Y. D. Zhang, "Direction-of-arrival estimation for coprime array via virtual array interpolation," *IEEE Transactions on Signal Processing*, vol. 66, no. 22, pp. 5956–5971, Nov 2018.
- [64] E. J. Candès and B. Recht, "Exact matrix completion via convex optimization," *Foundations of Computational Mathematics*, vol. 9, no. 6, p. 717, Apr 2009.
- [65] P. Stoica and A. Nehorai, "Music, maximum likelihood, and Cramer-Rao bound," *IEEE Transactions on Acoustics, Speech, and Signal Processing*, vol. 37, no. 5, pp. 720–741, May 1989.



Syed Ali Hamza received the PhD degree in electrical engineering from Villanova University, PA, USA in 2020. He is currently an Assistant Professor in the Department of Electrical Engineering, Widener University, PA, USA. His research interests are statistical and array signal processing, control systems and distributed signal processing for sensor networks.



Moeness Amin is a Fellow of the Institute of Electrical and Electronics Engineers; Fellow of the International Society of Optical Engineering; Fellow of the Institute of Engineering and Technology; and a Fellow of the European Association for Signal Processing. He is the Recipient of: the 2017 Fulbright Distinguished Chair in Advanced Science and Technology; the 2016 Alexander von Humboldt Research Award; the 2016 IET Achievement Medal; Recipient of the 2014 IEEE Signal Processing Society Technical Achievement Award; the 2009 Individual

Technical Achievement Award from the European Association for Signal Processing; the 2015 IEEE Aerospace and Electronic Systems Society Warren D White Award for Excellence in Radar Engineering; and the 2010 Chief of Naval Research Challenge Award. Dr. Amin is the Recipient of the IEEE Third Millennium Medal. He was a Distinguished Lecturer of the IEEE Signal Processing Society, 2003-2004, and is the past Chair of the Electrical Cluster of the Franklin Institute Committee on Science and the Arts. Dr. Amin has over 750 journal and conference publications in signal processing theory and applications, covering the areas of Wireless Communications, Radar, Sonar, Satellite Navigations, Ultrasound, Healthcare, and RFID. He has co-authored 21 book chapters and is the Editor of three books titled, *Through the Wall Radar Imaging*, *Compressive Sensing for Urban Radar*, *Radar for Indoor Monitoring*, published by CRC Press in 2011, 2014, 2017, respectively.